551·515·4 : 551·578·11

Thunderstorm rain *vs* steady precipitation from layer type clouds, as judged by study of raindrop sizes

R. C. SRIVASTAVA and R. K. KAPOOR

Rain and Cloud Physics Research Unit, C.S.I.R, New Delhi

ABSTRACT. Quantitatively reliable estimate by radar of precipitation intensity at a distance requires a critical prior study being made of drop size distribution in rain of various kinds and at different phases of rainfall. Observations in this regard have been made in two distinct types of radar synoptic situations—one associated predominantly with widespread continuous and relatively steady precipitation from cold stratiform clouds, and the other in which rain of a showery and more temporary and localised character occurs chiefly from very tall and highly supercooled clouds as in a thunderstorm. Some of the distinguishing features of drop size distribution and associated parameters, such as median volume diameter, total space concentration of drops, and radar reflectivity in the two situations are presented and discussed in the paper.

1. Introduction

Two of the most important objectives of determining drop size distributions in rain are—(1) helping elucidation of mechanisms of raindrop growth in clouds and (2) enabling estimate of rain intensities at a distance, on the basis of a certain dependable relationship connecting radar reflectivity, Z, and rainfall rate, R, as given by observed raindrop size spectra in different rain situations. Despite a large number of determinations of drop size spectrum in rain in different areas, it has not been possible till now to establish a clear cut relationship connecting drop size spectra and the basic process underlying rain formation in clouds in different meteorological situations. On the other hand, data of raindrop size distributions gathered in widely separated localities and in different rain situations, when averaged out, appear to be represented fairly uniformly, at least in the higher size ranges, by the following simple expression first proposed by Marshall and Palmer (1948)

$$N_D = N_0\, e^{-XD}, \qquad N_0 = 0\cdot08\ \text{cm}^{-4}$$

$$X = 41 R^{-0\cdot21}\ \text{cm}^{-4} \qquad (1)$$

where N_D is the number of drops of diameter D in unit volume of air per unit diameter range and X is a parameter which is related to rate of rainfall, R (mm/hr), by the second formula. As regards Z—R relationships, widely differing formulae have been reported (Twomey 1953) by different workers. In this connection, an attempt has been made by Atlas and Chmela (1957) to relate variations in Z—R relationship to synoptic situations. They have suggested that higher accuracy may be obtained in measurements of rainfall by radar, by using different Z—R equations in different synoptic situations, the Z—R equation used being related to synoptic situation in a physically consistent manner. In particular, they have shown that the coefficient and exponent in the relationship between Z(mm^6 m^{-3}) and R (mm/hr),

$$Z = 296\, R^{1\cdot47},$$

expected on the basis of Marshall-Palmer distribution would decrease and increase respectively, if the original Marshall-Palmer distribution is modified as a result of growth by coalescene with cloud droplets, while evaporation below cloud base would have the opposite effect.

In this note have been presented, raindrop size data collected in rains which are known from radar observations, to be pertaining to synoptic situations of different types, and their distinguishing features discussed in some detail.

2. Method of measurement and data collected

Raindrop size data designated in the note as belonging to rain situation of type A, have been collected on days on which observation by 3·2 cm meteorological radar at the Rain and Cloud Physics Centre, New Delhi showed widespread precipitation field giving echo with melting band. A pair of typical P.P.I. photographs of overhead scanning showing well-defined melting band, obtained on one such day, is shown in Fig. 1. Rain in such situations is usually of long duration and fairly steady in character. Drop size data denoted by type B have been collected on days on which radar observations revealed rain showers from tall convective clouds which did not exhibit any melting band feature, although the rain cell extended well above 0°C level. A typical P.P.I. and also an R.E.I. picture relating to one such rain situation of B-type is reproduced in Fig.2. Rain on such occasions is of relatively short duration and high intensity, and is characterised by marked fluctuations in rates of precipitation. While in the first case rain appears to be initiated by Bergeron-Findeisen mechanism, that in the second case is perhaps contributed largely by collision-coalescence process.

Raindrop size measurements have been made by exposing to rain Whatman No. 1 filter paper circles, with sampling area 675 sq. cm, for a known length of time, measuring sizes of impressions formed on the filter paper, and by relating these to original raindrop sizes on the basis of previous calibration. All raindrop size measurements have been grouped in diameter intervals of width 0·2 mm. Impressions of sizes less than that corresponding to raindrop diameter 0·4 mm or less have been neglected to avoid possible effects of drop shattering on impinging on the filter paper. In Tables 1(a) and 1(b) samples of each type are listed, together with date and time of measurements and certain other rain parameters.

3. Results and Discussions

An important single term parameter of drop size distribution in any given rain situation is the median volume diameter, D_0, this being so defined that drops of sizes less than D_0 constitute half the space concentration of rain water, the other half being contributed by drops of larger sizes. Assuming Marshall-Palmer distribution, this condition for median volume diameter may be expressed analytically by the relation—

$$\int_0^{\infty} D^3 e^{-XD} \; dD = 2\int_0^{D_0} D^3 e^{-XD} \; dD,$$

which, after integration, yields

$$(XD_0)^3 + 3(XD_0)^2 + 6(XD_0) + 6 = 3\, e^{XD_0}$$

This equation is satisfied by

$$D_0 = 3 \cdot 67/X$$

The Marshall-Palmer distribution (1) may consequently be written in the alternative form

$$N_D = N_0\, e^{-\lambda D/D_0}, \quad \lambda = 3\cdot 67 \qquad (2)$$

in terms of the dimensionless scaled diameter D/D_0. In this form the parameter X, depending upon rainfall intensity, is replaced by the parameter D_0.

As will be seen, according to equation (2), a plot of N_D *vs* D/D_0 on a simple log scale would be represented by a straight line which would intercept the N_D axis at the point $N_D = N_0$. Plotting values as obtained from individual samples, it is, however, seen that although the curves conform reasonably well to this straight line characteristic, intercepts on N_D axis differ widely in many of the cases and the slope of the line also departs from the theoretically expected value of $\lambda = 3\cdot 67$. An idea of the nature of variations shown by different samples can be had from values of N_0/λ listed in the last column of Tables 1 (a) and 1(b). N_0/λ has been calculated by

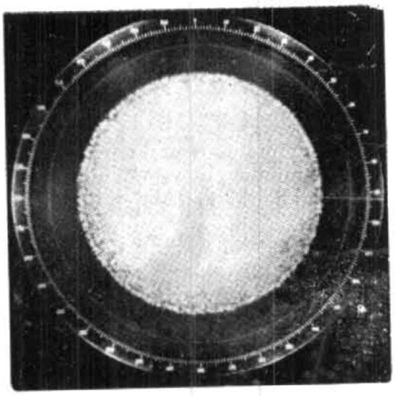

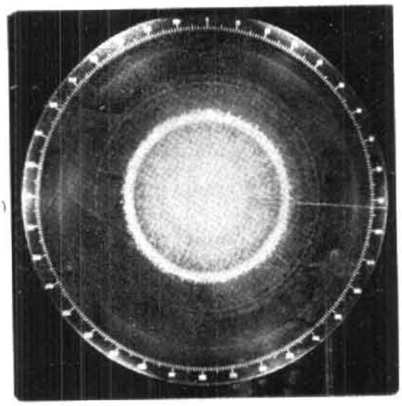

Fig. 1. Overhead P.P.I. pictures at 90° elevation, taking at high and low receiver gain, showing well defined melting band

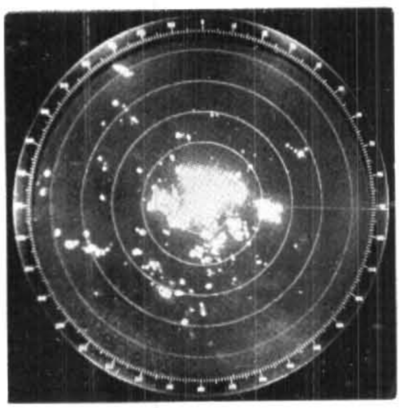

Fig. 2(a). P.P.I. picture (range 100 km, elevation 2·5°) showing convective rain cells on 27 July 1959

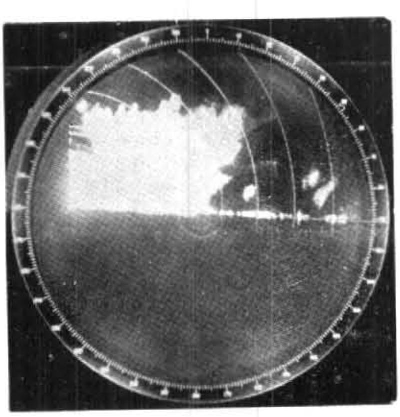

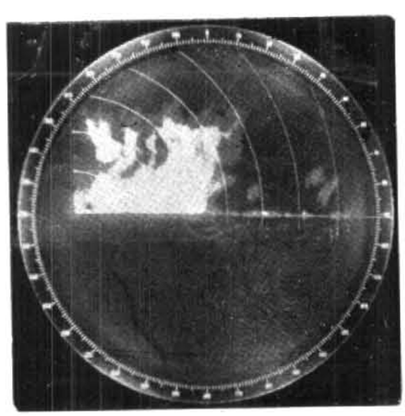

Fig. 2(b) Fig. 2(c)

R.E.I. pictures (range 20 km), at high and low receiver gain, show no melting band feature in cold convective cells on 27 July 1959

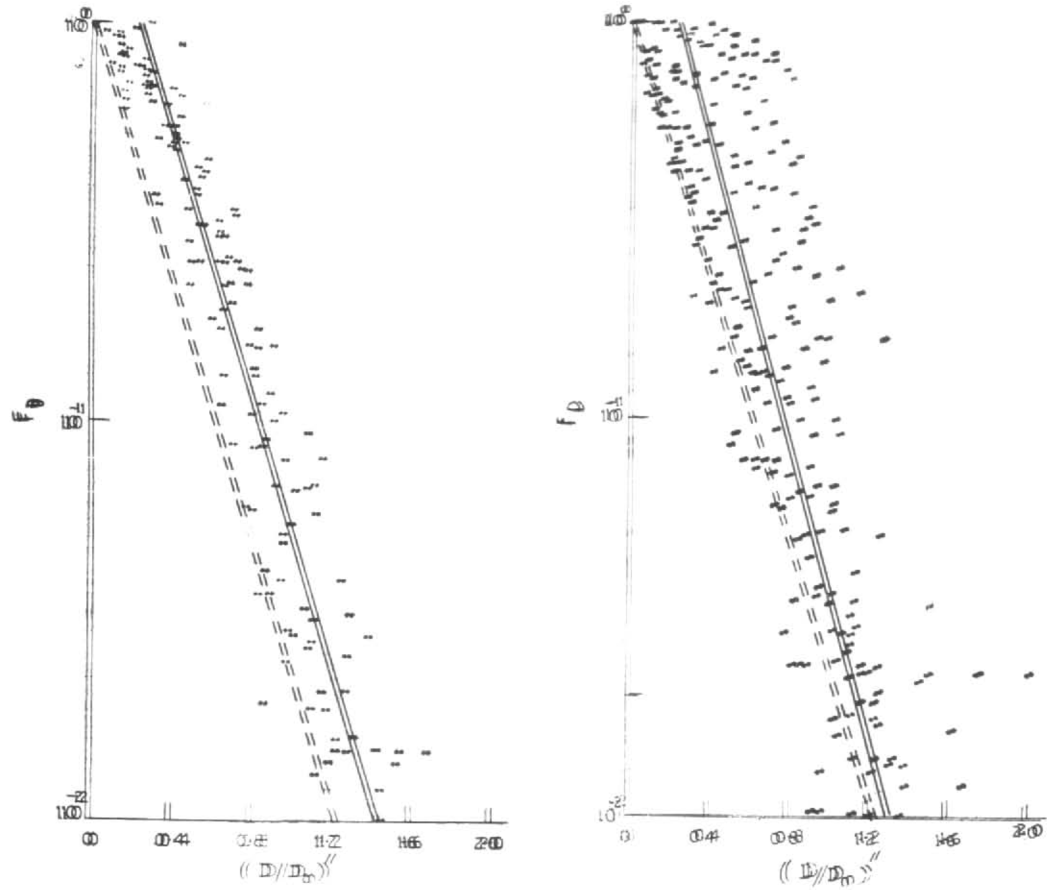

Fig. 3(a). A-type

Fig. 3(b). B-type

Fig. 3. Dot diagrams of F_D vs $(D/D_0)'$ for A-type (16 samples) and B-type (18 samples) rain situations

integrating equation (2) as below

$$\int_{0.4}^{\infty} N_0 \, e^{-\lambda D/D_0} \, dD = \frac{N_0 D_0}{\lambda} \, e^{-0\cdot 4\lambda/D_0} = n_{0\cdot 4}$$

where $n_{0\cdot 4}$ gives the total number of raindrops recorded.

From this we get $\frac{N_0}{\lambda} = \frac{n_{0\cdot 4}}{D_0} \, e^{0\cdot 4\lambda/D_0}$

Taking, as a first approximation, that λ occurring in the exponential is equal to $3\cdot 67$, the various values of N_0/λ have been calculated from the above equation. The values obtained are found to vary from $21\cdot 4\times 10^3$ to $1\cdot 62\times 10^3$ in case of raindrop spectra of type A, and from $1\cdot 05\times 10^3$ to $3\cdot 71\times 10^3$ for spectra of B-type , as against a constant value of $2\cdot 18\times 10^3$ expected on the basis of equation (2). Observed variations are seen to be larger in case of samples of B-type, some of the lowest values obtained being associated with samples collected during initial phases of convective rain showers, with correspondingly rather abnormally high values of D_0.

To help eliminate scatter of $N_D - D/D_0$ plots, as might be due to variations in values of N_0/λ from sample to sample, the parameter relating to drop number has been normalized by adopting the following procedure. The cumulative number of drops, n_D , with diameters equal to D or larger than D is expressed as a fraction, F_D, of total number of drops recorded. If drop size distribution in each individual sample conformed generally to Marshall-Palmer distribution, and N_0/λ only varied from sample to sample, F_D would be related to D by the following equation

$$F_D = \frac{\int_{D}^{\infty} N_0 \, e^{-\lambda . D/D_0} \, dD}{\int_{0\cdot 4}^{\infty} N_0 \, e^{-\lambda . D/D_0} \, dD}$$

Or $$F_D = e^{-\lambda\cdot(D/D_0)'} \qquad (3)$$

where

$(D/D_0)'$ is written in place of $\left(\frac{D-0\cdot 4}{D_0}\right)$.

Plots on a simple log scale of F_D against $(D/D_0)'$ relating to samples collected in various A and B-type rain situations are shown in Figs. 3(a) and 3(b). In these diagrams, the straight line given by equation (3) is shown by a dashed line while the best straight line fit of actual data, as estimated by eye, is shown in full lines. Comparing the plots relating to the two types of rain situations it is seen that the scatter is much more pronounced in case of showery precipitation as on B-type days. From the comparative regularity of distribution of points relating to a A-type rain it would appear that the process of rain formation by Bergeron or ice-mechanism leading to drop size distribution in rain from cold layer type clouds is, on the whole, a more systematic process, leading to better agreement in observed drop size distributions in rain on different occasions. The line of best fit for A-type samples runs more or less parallel to the line represented by equation (3), while that relating to B-type samples slopes somewhat more steeply, giving a mean value of $\lambda = 4\cdot 25$ as against theoretical value of $3\cdot 67$. The fractional number of drops falls off more sharply with scaled diameter in thundery rain of type B compared with that in steady type precipitation in A-type rain situations. Intercepts on the F_D axis in case of A-type and B-type spectra are $2\cdot 16$ and $2\cdot 59$ respectively.

Plotting F_D against $(D/D_0)'$ as given by individual samples it is seen that while in general spectra of both types are well represented by a combination of two straight lines having different slopes, this feature of distribution is more regular in case of A-type rain. Four typical rain samples of each type plotted in this way are shown in Figs. 4(a) and 4(b), the abscissae being shifted by $0\cdot 8$ units for each successive sample.

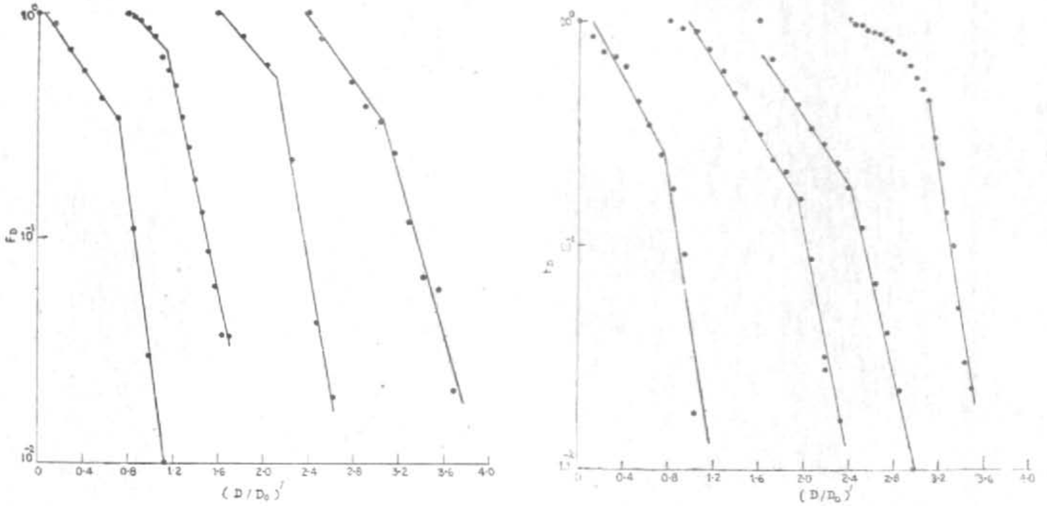

Fig. 4(a). A-type

Fig. 4(b). B-type

Fig. 4. Plots of F_D *vs* $(D/D_0)'$ for four individual samples of each type

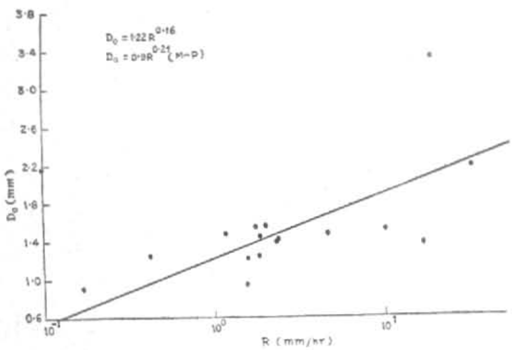

Fig. 5(a). Dot diagram of D_0 *vs* R for A-type rain spectra

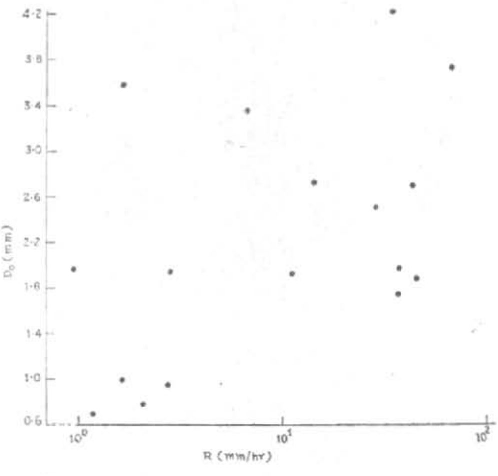

Fig. 5(b). Dot diagram of D_0 *vs* R for B-type rain spectra

If number of drops above 0·4 mm diameter and median volume diameter could be related to rainfall intensity we would be in a position, by using equation (3), to derive a certain unique relationship connecting rain intensities and drop size distributions. Plots of R againt D_0 in the two types of rain situations are as shown in Figs. 5(a) and 5(b). It is seen that while the correlation is rather poor in case of B-type samples the two elements can be fairly well represented by the equation

$$D_0 = 1{\cdot}22\,R^{0\cdot16} \qquad (4)$$

in case of A-type rain. This may be compared with the theoretical value

$$D_0 = 0{\cdot}9\,R^{0\cdot21}$$

on the basis of Marshall-Palmer distribution.

Again, plotting on double log scales $n_{0\cdot4}$ against R, we notice a certain regularity in the distribution of points in case of A-type spectra (Fig. 6a), with the line of least squares fit being given by

$$n_{0\cdot4} = 78\,R^{0\cdot47} \qquad (5)$$

Plots relating to B-type rain (Fig. 6b), on the other hand, show a considerable degree of scatter and do not justify drawing any line of best fit.

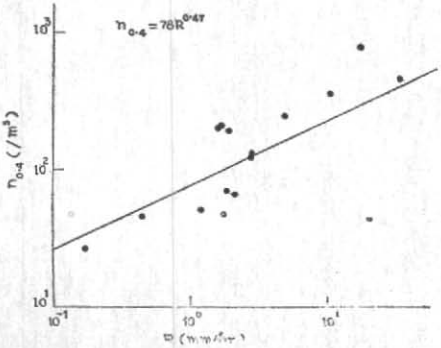

Fig. 6(a). A-type rain situation

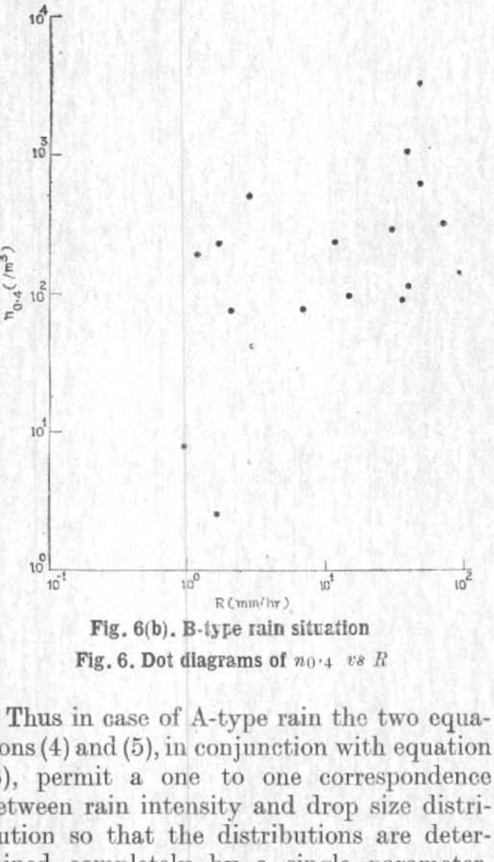

Fig. 6(b). B-type rain situation

Fig. 6. Dot diagrams of $n_{0\cdot4}$ *vs* R

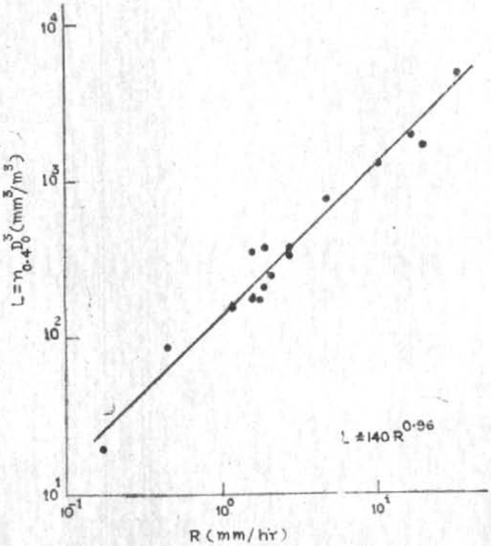

Fig. 7(a). A-type rain sample

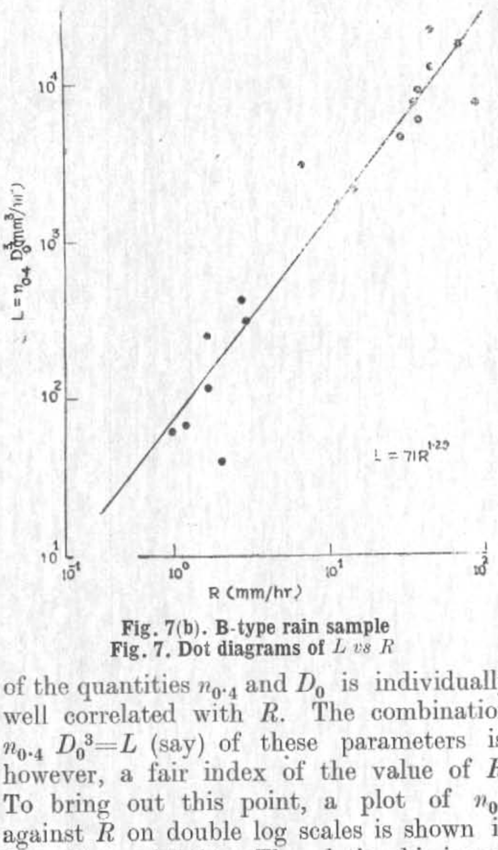

Fig. 7(b). B-type rain sample

Fig. 7. Dot diagrams of L *vs* R

Thus in case of A-type rain the two equations (4) and (5), in conjunction with equation (3), permit a one to one correspondence between rain intensity and drop size distribution so that the distributions are determined completely by a single parameter. In case of B-type rain it is apparent, on the other hand, that both the parameters, $n_{0\cdot4}$ and D_0, are necessary for complete specification of drop size distribution since neither of the quantities $n_{0\cdot4}$ and D_0 is individually well correlated with R. The combination $n_{0\cdot4}\ D_0^3 = L$ (say) of these parameters is, however, a fair index of the value of R. To bring out this point, a plot of $n_{0\cdot4}$ against R on double log scales is shown in Figs. 7(a) and 7 (b). The relationship is seen

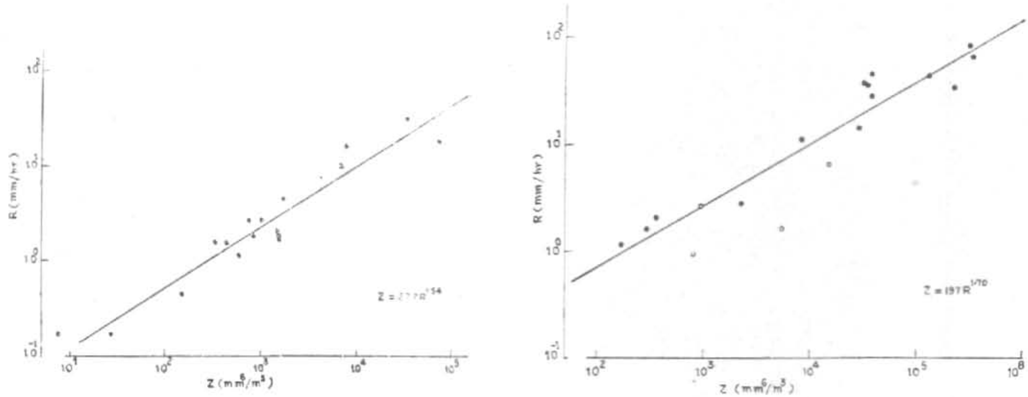

Fig. 8(a). A-type

Fig. 8(b). B-type

Fig. 8. Dot diagrams showing relationship between Z and R for A-type and B-type rain spectra

Open circles in Fig. 8(b) pertain to samples collected during initial phases of shower processes

TABLE 1(a)

A-type samples

Date	Time (IST)	R (mm/hr)	D_0 (mm)	$n_{0 \cdot 4}$ (per m^3)	N_0/λ (m^{-3}mm^{-1})
7-7-1959	1206	2·77	1·41	$1 \cdot 34 \times 10^{2}$	$2 \cdot 69 \times 10^{2}$
	1211	1·56	0·93	$2 \cdot 18 \times 10^{2}$	$1 \cdot 14 \times 10^{3}$
18-7-1959	1025	1·74	1·54	$4 \cdot 79 \times 10^{1}$	$8 \cdot 05 \times 10^{1}$
	1030	1·86	1·43	$7 \cdot 08 \times 10^{1}$	$1 \cdot 39 \times 10^{2}$
	1035	1·18	1·46	$5 \cdot 10 \times 10^{1}$	$9 \cdot 59 \times 10^{1}$
	1044	2·02	1·55	$6 \cdot 60 \times 10^{1}$	$1 \cdot 10 \times 10^{2}$
	1053	0·44	1·24	$4 \cdot 64 \times 10^{1}$	$1 \cdot 22 \times 10^{2}$
	1119	0·17	0·90	$2 \cdot 67 \times 10^{1}$	$1 \cdot 52 \times 10^{2}$
1-8-1959	1027	2·68	1·38	$1 \cdot 26 \times 10^{2}$	$2 \cdot 64 \times 10^{2}$
	1100	19·43	3·32	$4 \cdot 57 \times 10^{1}$	$2 \cdot 14 \times 10^{1}$
13-8-1959	1143	32·80	2·17	$4 \cdot 79 \times 10^{2}$	$4 \cdot 37 \times 10^{2}$
	1150	16·90	1·37	$7 \cdot 62 \times 10^{2}$	$1 \cdot 62 \times 10^{3}$
6-9-1959	1013	10·03	1·51	$3 \cdot 72 \times 10^{2}$	$6 \cdot 50 \times 10^{2}$
	1020	4·69	1·46	$2 \cdot 55 \times 10^{2}$	$4 \cdot 78 \times 10^{2}$
	1028	1·84	1·23	$1 \cdot 99 \times 10^{2}$	$5 \cdot 29 \times 10^{2}$
	1035	1·56	1·21	$2 \cdot 03 \times 10^{2}$	$5 \cdot 64 \times 10^{2}$

TABLE 1(b)

B type samples

Date	Time (IST)	R (mm/hr)	D_0 (mm)	$n_{0\cdot4}$ (per m³)	N_0/λ ($m^{-3}mm^{-1}$)
20-7-1959	1558	2·82	1·94	$4\cdot24\times10^1$	$4\cdot69\times10^1$
	1610	6·73	3·36	$7\cdot96\times10^1$	$1\cdot00\times10^2$
	1611	45·80	1·89	$3\cdot21\times10^3$	$3\cdot71\times10^3$
		44·80	2·71	$6\cdot30\times10^2$	$3\cdot99\times10^2$
25-7-1959	1020	1·68	3·59	2·5	1·05
	1024	0·95	1·97	7·91	8·52
	1026	29·90	2·51	$2\cdot90\times10^2$	$2\cdot07\times10^2$
	1055	1·64	1·02	$2\cdot34\times10^2$	$9\cdot68\times10^2$
27-7-1959	1050	2·74	0·95	$5\cdot05\times10^2$	$1\cdot21\times10^3$
	1158	14·41	2·73	$1\cdot01\times10^2$	$6\cdot36\times10^1$
	1338	36·80	1·75	$1\cdot06\times10^3$	$1\cdot41\times10^3$
3-8-1959	1310	86·10	3·66	$1\cdot45\times10^2$	$5\cdot91\times10^1$
	1315	35·10	4·26	$9\cdot31\times10^1$	$3\cdot06\times10^1$
	1323	2·08	0·79	$7\text{-}88\times10^1$	$6\cdot41\times10^2$
	1334	1·18	0·70	$1\cdot92\times10^2$	$2\cdot24\times10^3$
8-9-1959	1000	68·60	3·74	$3\cdot30\times10^2$	$1\cdot30\times10^2$
	1007	37·50	1·98	$1\cdot14\times10^2$	$1\cdot21\times10^3$
	1012	11·27	1·93	$2\cdot36\times10^2$	$2\cdot61\times10^2$

to be good in case of B as well as A-type rains, the lines of best fit being

$$\left.\begin{array}{ll} L=140\,R^{0.96} & \text{(Type A)} \\ L=71\,R^{1.29} & \text{(Type B)} \end{array}\right\} \qquad (6)$$

The second equation of the above set in conjunction with equation (3) enables us to establish a connection between drop size distribution in B-type rain and any two of the parameters $n_{0\cdot4}$, D_0 and R. It is seen from these formulae and also directly from Fig. 7, that for the same low intensity rainfall, represented by the same median volume diameters, the number of drops, $n_{0\cdot4}$, is smaller in case of type B rain. On the other hand, if the number of drops, $n_{0\cdot4}$, is the same, D_0 is lower in case of type B spectra. The position, however, appears to get reversed for intensities greater than 8 mm/hr.

A plot of radar reflectivity, $Z = \Sigma N_D D^6\,\delta D$ againt R for the two types of rain situations together with the lines of best fit,

$$Z=277\,R^{1.54} \qquad \text{(Type A)} \qquad 7(a)$$

$$Z=197\,R^{1.70} \qquad \text{(Type B)} \qquad 7(b)$$

as calculated by method of least squares, is shown in Figs. 8(a) and 8(b). The equation for A-type distributions is seen to be in good agreement with that expected on the basis of Marshall-Palmer distribution,

$$Z=296\ R^{1.47}.$$

Smaller value of the coefficient and larger value of the exponent in equation 7(b) points to larger influence of coalescence process in growth of raindrops in case of type B spectra.

Further, equations (7) show that for low intensities of rainfall (upto about 13 mm/hr)

Z is smaller in case of B-type rain, the features being just the opposite for higher intensities of rainfall. This may partly be due to the fact that low intensity rainfall in case of thundery type rain is commonly associated with samples taken towards the end stages of shower processes. A glance at Fig.8(b), in which points corresponding to initial phases of shower processes have been depicted by open circles, will show that for the same rainfall intensity samples collected at the initial phases show higher Z as compared to samples collected at the end stages. This is in agreement with the common observation that at the initial stages of convective showers drops of relatively large-sizes predominate. Further observations are, however, necessary to permit any firm generalization in this regard.

4. Concluding remarks

The drop size distribution and associated parameters point unmistakably to the more systematic nature of type A spectra. Observed larger degree of variability of spectral character in case of rain from convective clouds is the result apparently of more changeable nature of showery type precipitation from such clouds. It is felt that further study of type B spectra, with particular reference to the various phases of precipitation, would be of value in resolving some of the observed variations in the nature of drop size distributions from one situation to another.

5. Acknowledgements

The authors wish to record their grateful thanks to the Radar Laboratory of Rain and Cloud Physics Research Centre for making available the radar observations used in this study. They are also thankful to Shri L.T. Khemani for help in raindrop size observation and computation of data.

REFERENCES

Atlas, D. and Chmela, A. C. 1957 *Proc. Sixth Weath. Radar Conf.*, p. 21.

Marshall, J. S. and Palmer, W. Mck. 1948 *J. Met.*, **5**, p. 165.

Twomey, S. 1953 *Ibid.*, **10**, p. 66.